




# Tricuspid regurgitation: recent advances in understanding pathophysiology, severity grading and outcome

Rebecca T. Hahn <sup>1\*</sup>, Luigi P. Badano<sup>2,3</sup>, Philipp E. Bartko<sup>4</sup>, Denisa Muraru <sup>2,3</sup>,  
Francesco Maisano<sup>5</sup>, Jose L. Zamorano<sup>6</sup> and Erwan Donal <sup>7</sup>

<sup>1</sup>Cardiology Department, NewYork-Presbyterian/Columbia University Medical Center, 177 Fort Washington Avenue, New York, NY 10032, USA; <sup>2</sup>Department of Medicine and Surgery, University of Milano-Bicocca, Milan, Italy; <sup>3</sup>Department of Cardiological, Neural and Metabolic Sciences, Istituto Auxologico Italiano, IRCCS, San Luca Hospital, Milan, Italy; <sup>4</sup>Department of Internal Medicine II, Medical University of Vienna, Vienna, Austria; <sup>5</sup>Department of Cardiothoracic Surgery, IRCCS Ospedale San Raffaele, Milano, Italy; <sup>6</sup>Cardiology Department, University Hospital Ramón y Cajal, Madrid, Spain; Instituto Ramón y Cajal de Investigación Sanitaria (IRYCIS), Madrid, Spain; and <sup>7</sup>Cardiology Department, Université de Rennes-1, Rennes, France

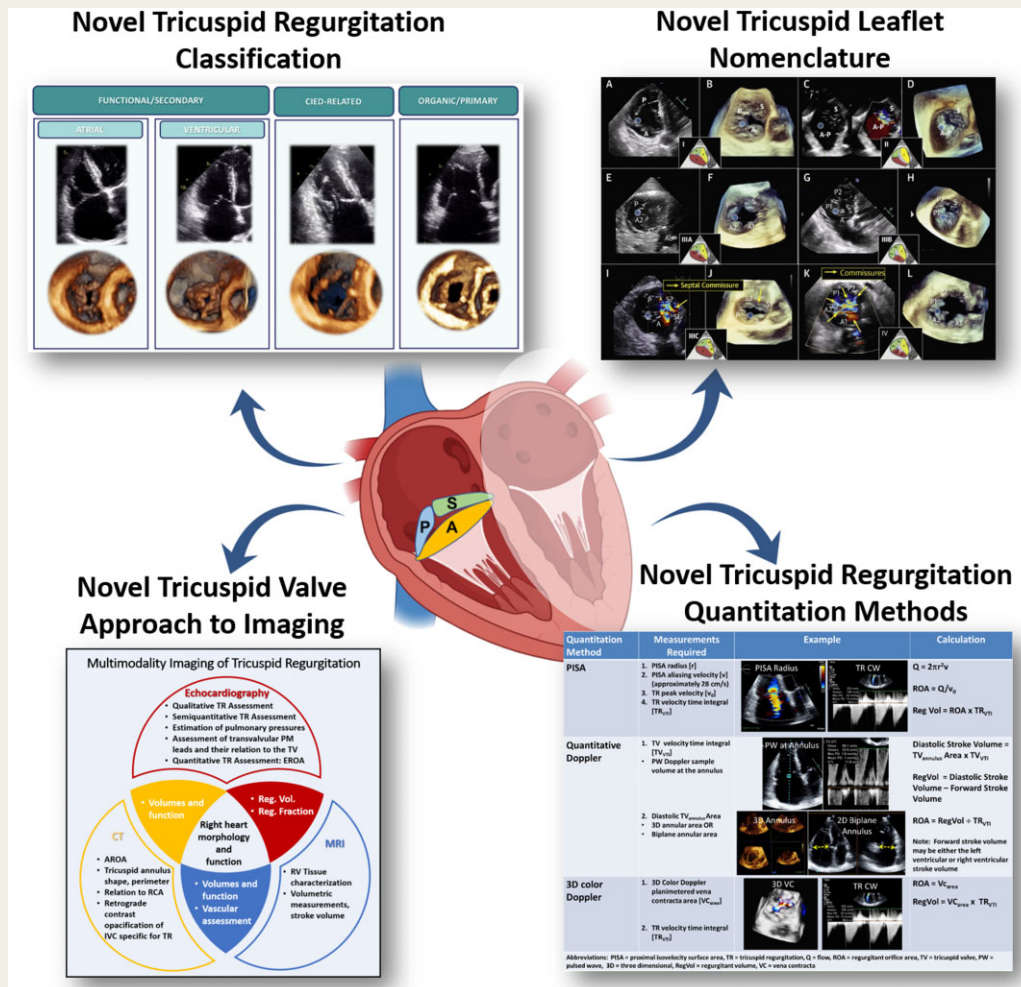
Received 6 December 2021; revised 5 January 2022; editorial decision 8 January 2022; accepted 11 January 2022; online publish-ahead-of-print 14 February 2022

Heightened interest in tricuspid regurgitation (TR) stems from the consistent association of mortality with greater severity of TR, and a low use of surgical solutions in the setting of high in-hospital mortality attributed to the late presentation of the disease. The delay in intervention is likely related to a limited understanding of the valvular/ventricular anatomy and disease pathophysiology, along with an underestimation of TR severity by standard imaging modalities. With the rapid development of transcatheter solutions which have shown early safety and efficacy, there is a growing need to understand and accurately diagnose the valvular disease process in order to determine appropriate management solutions. The current review will describe both normal and pathologic tricuspid valvular anatomy, the classification of these anatomic substrates of TR, the strengths and limitations of the current guidelines-recommended multi-parametric echocardiographic approach and the role of multi-modality imaging, as well as the role of transcatheter device therapy in the management of the disease.

\* Corresponding author. Tel: +1 212 342 0444; Fax: +1 646 426 0204. E-mail: [rth2@columbia.edu](mailto:rth2@columbia.edu)

Published on behalf of the European Society of Cardiology. All rights reserved. © The Author(s) 2022. For permissions, please email: [journals.permissions@oup.com](mailto:journals.permissions@oup.com).

Graphical Abstract



Heightened interest in tricuspid regurgitation (TR) has led to a novel classification of the aetiology of TR, novel leaflet nomenclature, novel ways of quantifying TR, and novel methods for imaging the tricuspid valve complex.

**Keywords** tricuspid valve • tricuspid regurgitation • transcatheter

**Introduction**

Heightened interest in tricuspid regurgitation (TR), the previously ‘forgotten valve’, may be related to consistent findings in three main areas. First, multiple studies show an independent association of mortality with higher grades of TR severity.<sup>1,2</sup> Second, isolated surgical intervention for TR is infrequently performed<sup>3</sup> and associated with ~8–10% in-hospital mortality.<sup>4,5</sup> Third, the early success of transcatheter repair<sup>6</sup> and replacement<sup>7</sup> techniques has increase access to relatively low-risk treatments.

The current review will describe both normal and pathologic tricuspid valvular (TV) anatomy, the classification of the anatomic substrates of TR, and the strengths and limitations of the current guidelines-recommended multi-parametric echocardiographic

approach as well as new methods and algorithms to determining TR severity.<sup>8–12</sup> The role of transcatheter device therapy will also be discussed.

**Tricuspid valve anatomy**

**Tricuspid valve leaflets**

The TV is typically composed of three leaflets of unequal size which by convention are named the anterior, posterior, and septal leaflets. However, this convention is based on a vertical position of the long axis of the heart. Whereas by positioning the TV in the anatomic or ‘attitudinal’ position, with the long axis rotated counterclockwise from vertical, the anterior leaflet is anterior–superior, the posterior

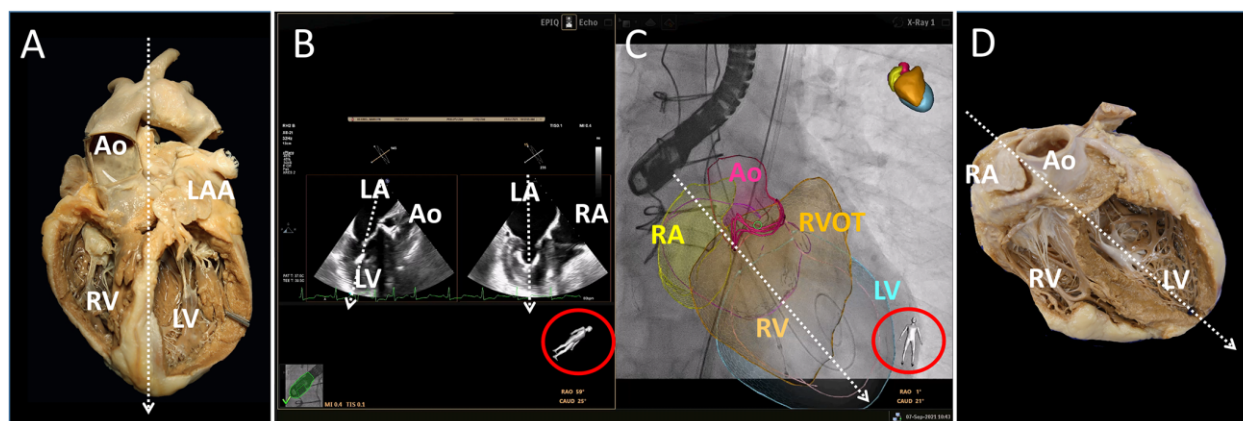


**Figure 1** Vertical versus anatomic imaging of the heart. (A) A gross anatomic specimen in the vertical or “valentine” position which is typically obtained with the transoesophageal (TOE) probe behind the dome of the left atrium (panel B) and with the apex of the heart in the far field of imaging. The human model (B, red circle) is oriented to the on-screen TOE image, confirming the valentine position. (C) The fluoroscopic view of the patient with fusion of the segmented 3D TOE volume. The imaging plane of the TOE (white dashed arrow) is along the long-axis of heart generating the valentine view, however the fluoroscopic view is an anterior-posterior projection as shown human model (C, red circle) which generates an attitudinal view (Panel D). The conventional naming system of anterior, posterior and septal leaflets, would become in the attitudinal view, the anterior-superior, inferior and posterior leaflet. Ao = aorta, LAA = left atrial appendage, LA = left atrium, LV = left ventricle, RA = right atrium, RV = right ventricle, RVOT = right ventricular outflow tract.

leaflet is inferior, and the septal leaflet is posterior (Figure 1).<sup>13</sup> The attitudinal position will determine the direction of intra-cardiac catheters during transcatheter procedures.<sup>14</sup> However, there are multiple reasons to maintain the original nomenclature of anterior, posterior and septal leaflets. This nomenclature is derived from the traditional “surgical view” approach used for many years to enhance communication between imagers and surgeons. Similarly, transcatheter interventions will be performed using echocardiographic guidance and clear communication between imager and interventionalist is essential. By naming the TV leaflets based on consistent intra-cardiac anatomy (interventricular septum for the septal leaflet, anterior to the aorta for the anterior leaflet, and posterior to the anterolateral papillary muscle for the posterior leaflet) one maintains a common language that can be used with all imaging modalities, and improves consistent communication within procedures, irrespective of individual attitudinal variability. In the classic three leaflet valve, the anterior and septal leaflets are usually the largest circumferentially, thus the anteroseptal commissure is the longest.<sup>15</sup> There are typically two distinct papillary muscles (anterior, posterior), and a third variable septal papillary muscle. The anterior papillary muscle is the largest and provides chordae to the anterior and posterior leaflets. It arises from the anterior/lateral wall of the right ventricle (RV), near the trabeculations which incorporate the moderator band.<sup>16</sup>

Pathology studies have long recognized that there are a variable number of leaflets in healthy subjects<sup>17,18</sup> but use varying terminology to describe these supernumerary leaflets.<sup>19,20</sup> Recently a simplified nomenclature has been proposed<sup>21</sup> which may be relevant to pre-procedural planning and execution of transcatheter devices<sup>22</sup> as well as determine device success.<sup>22,23</sup> Given the proximity of the TV to the anterior chest wall and diaphragm, identification of the leaflet morphologies can be

performed on either 2D transthoracic echocardiography (TTE) from modified views or 2D transoesophageal echocardiographic (TOE) transgastric short-axis view, or the 3D volume-rendered equivalent using either modality. In this nomenclature proposal, deep indentations and true commissures were considered anatomically equivalent and were used to identify supernumerary leaflets. This convention can be justified by the observation that both folds in the leaflets or true commissures are accompanied by greater numbers of chordae along the leaflet edges and create potential sites for malcoaptation of the leaflet edges. A separate leaflet was then defined by: (i) independent motion from the adjacent leaflet, and (ii) colour Doppler flow in systole extending into the region around the leaflet. Four major classes of leaflet morphologies are shown in Figure 2: Type I is the classic 3-leaflet morphology; Type II is the 2-leaflet morphology with fusion of the anterior and posterior leaflets; Type III is the 4-leaflet configuration with subcategories based on the location of the fourth leaflet; and Type IV has >4 leaflets.

Leaflet structure and function can be used to categorize TR: (i) pathologic changes to the leaflets resulting in leaflet defects or malcoaptation, referred to as primary TR; (ii) insufficient leaflet coverage of a dilated tricuspid annulus (TA), referred to as atrial secondary TR, and (iii) insufficient leaflet coaptation in the setting of apical displacement with leaflet tethering, referred to as ventricular secondary TR (Table 1, Figure 3). Atrial secondary TR has been associated with marked right atrial (RA) and TA dilatation, typically less tethering or tenting of the tricuspid leaflets, and with normal or mildly dilated RV showing more triangular shape and preserved function.<sup>24–26</sup> Although cardiac implantable electronic device (CIED) leads have been traditionally categorized as primary because of the direct effect on the leaflets or subvalvular apparatus, there is nonetheless a

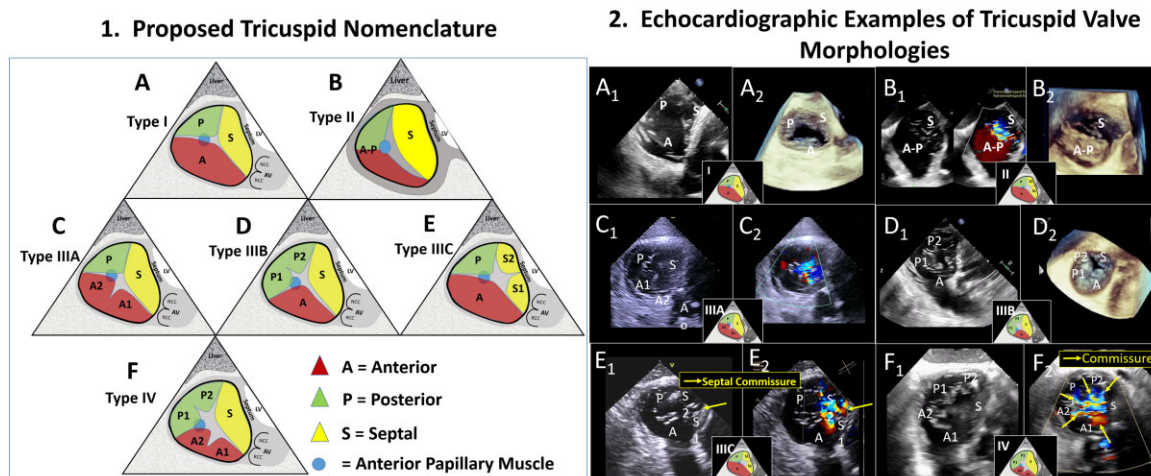


**Figure 2** Tricuspid valve nomenclature classification scheme. A proposed Tricuspid Valve Nomenclature Classification scheme is shown in the left panel (1). The anterior papillary muscle is indicated as a blue circle and defines the separation of the anterior from the posterior leaflets. (A) The Type I, 3-leaflet configuration. (B) The Type II, 2-leaflet configuration. (C and D) The Type III, 4-leaflet configurations. (F) The Type IV, 5-leaflet configuration. The panel on the right (2), shows echocardiographic examples of the tricuspid valve morphologies and the letter labels correspond to the proposed nomenclature in the left panel. (A1 and A2) Type I morphology by 2D and 3D imaging. (B1 and B2) Type II morphology by 2D and 3D imaging. (C1 and C2) Type IIIA morphology by 2D imaging without and with color Doppler. (D1 and D2) Type IIIB morphology by 2D and 3D imaging. (E1 and E2) Type IIIC morphology by 2D imaging without and with color Doppler. (F1 and F2) Type IV morphology by 2D imaging without and with color Doppler. Abbreviations: 2D = two dimensional, 3D = three-dimensional, A = anterior leaflet, P = posterior leaflet, S = septal leaflet, LV = left ventricle, AV = aortic valve, NCC = non-coronary cusp, RCC = right coronary cusp. Reproduced with permission from Hahn et al.<sup>21</sup>

'device' in place making the resulting TR a complication secondary to the CIED leads.

## Tricuspid annulus

The TV is a complex of interconnected components that includes leaflets hinged at the atrioventricular junction and suspended by tendinous chords (chordae tendineae) attached to the ventricular septum or to papillary muscles that in turn arise from the ventricular wall. At the hinge of the leaflets, RA myocardium may overlap the leaflet surface by 0.5–2 mm. Thus, normal valvular function requires not only normality of all the valvular components but also adjoining RA and RV walls for sphincteric contraction and excursion of the orifice towards the ventricular apex, as well as interaction with the left ventricle through muscular continuity. Anatomically, the fibrous TA is indistinct and incomplete, especially at the segment corresponding to the RV-free wall accounting for the potential dilatation in these regions, as opposed to the septal region. The TA is almost oval and is non-planar but becomes more circular as the RV dilates. Furthermore, its geometry can also be distorted by dilatation of the RA and/or RV<sup>27</sup> and aortic root.<sup>28,29</sup>

The TA is highly dynamic during the cardiac cycle, and the interaction between the TA dimensions, leaflet coaptation and TR severity, contribute to patient prognosis.<sup>30,31</sup> TA size is variable in the different cardiac phases and should increase from end-systole to end-diastole, whereas TA shape is more consistent throughout the cardiac cycle. Addetia et al.<sup>32</sup> demonstrated that the TA size measured with 3D TTE may change ~30% between systole and diastole. In comparison, Ton-Nu et al.<sup>33</sup> demonstrated that patients with significant secondary TR

had larger, more planar, and circular geometry of TA compared with controls using 3DE. Using cardiac computed tomography, Hirasawa et al.<sup>34</sup> demonstrated that circular remodelling of the TA shape at end-diastole (anteroposterior/septolateral ratio < 1.20) is associated with more RA and RV dilation, and a higher long-term mortality.

Identification of the main pathogenic mechanism for TR might have prognostic implications.<sup>35</sup> Min et al.<sup>36</sup> demonstrated that the anteroposterior annulus diameter and tenting volume before tricuspid annuloplasty were independent predictors of residual TR after surgical correction. When using 2D TTE, the TA diameter should be measured at end-diastole on an apical four-chamber view and TA dilation is defined as a TA diameter  $\geq 40$  mm or  $> 21$  mm/m<sup>2</sup>. However, due to the non-circular shape of the TA, small rotations of the probe can result in significant changes of the linear dimensions.<sup>37</sup> Moreover, TA dimensions and shape change significantly along with the cardiac cycle and the evidence supporting the assessment of the TA at end-diastole is very limited.<sup>25,38</sup> Finally, atrial fibrillation (AFib) is associated with large beat-to-beat variation of TA dimension.<sup>39</sup>

## Classification of tricuspid regurgitation

The most commonly used classification of TR uses leaflet involvement to stratify patients into two broad categories of primary disease (leaflet pathology) or the secondary disease (non-leaflet pathology, Table 1. For many years, secondary TR has been considered a unique entity that—as opposed to primary TR—is predominantly

**Table 1** Classification of tricuspid regurgitation (TR).

Classification	Etiologies
<b>Structural abnormality of the tricuspid valve apparatus</b>	
<b>Primary TR: ~10-15% of patients</b>	
<b>Degenerative Disease</b>	<ul style="list-style-type: none"> <li>• Prolapse</li> <li>• Flail</li> </ul>
<b>Congenital</b>	<ul style="list-style-type: none"> <li>• Ebstein's Anomaly</li> <li>• Leaflet clefts</li> </ul>
<b>Acquired</b>	<ul style="list-style-type: none"> <li>• Rheumatic disease (usually with left-side disease)</li> <li>• Infective endocarditis</li> <li>• Endomyocardial fibrosis</li> <li>• Carcinoid disease, serotonin active drugs</li> <li>• Traumatic (blunt chest injury, laceration)</li> <li>• Iatrogenic <ul style="list-style-type: none"> <li>• Right ventricular biopsy</li> <li>• Drugs (e.g. exposure to fenfluramine-phentermine, or methysergide)</li> </ul> </li> </ul>
Radiation therapy of the mediastinum	
<b>Morphological normal leaflets with annular dilatation and/or leaflet tethering</b>	
<b>Functional TR: ~ 80% of patients</b>	
<b>Ventricular secondary TR</b>	<ul style="list-style-type: none"> <li>• Left heart diseases (left ventricular dysfunction or left heart valve diseases) resulting in pulmonary hypertension</li> <li>• Primary pulmonary hypertension</li> <li>• Secondary pulmonary hypertension (e.g. chronic lung disease, pulmonary thromboembolism, left-to-right shunt)</li> <li>• Right ventricular dysfunction from any cause (e.g. myocardial diseases, ischemic heart disease, chronic right ventricular pacing)</li> </ul>
<b>Atrial secondary TR</b>	<ul style="list-style-type: none"> <li>• Atrial fibrillation</li> <li>• Heart Failure with preserved ejection fraction</li> </ul>
<b>Cardiac tumors (particularly right atrial myxomas)</b>	<ul style="list-style-type: none"> <li>• Right atrial myxomas</li> </ul>
<b>Cardiac implantable electronic device (CIED) induced TR (~ 5% of patients)</b>	
<b>Primary CIED-induced TR</b>	<ul style="list-style-type: none"> <li>• CIED caused by direct interaction of the lead on the valve leaflets)</li> </ul>
<b>Secondary CIED-induced TR</b>	<ul style="list-style-type: none"> <li>• Incidental CIED, with TR due to functional etiologies or pacing related remodeling</li> </ul>

characterized by the structural integrity of the TV leaflets and is caused by RV remodelling following pressure and/or volume overload.<sup>38</sup> Based on its predominant imaging features, secondary TR may also be described in a practical way using Carpentier's functional classification based on leaflet mobility. Accordingly, Carpentier type I corresponds to normal leaflet motion and predominant TA dilation, as seen in atrial secondary TR. Carpentier type IIIb corresponds to leaflet tethering with restricted motion in systole, as typically seen in ventricular secondary TR. All types of Carpentier classification can be

encountered in primary TR and in CIED-induced TR, in which leaflet mobility may be highly variable depending on the aetiology. However, Carpentier classification was originally intended to guide mitral valve surgical repair or replacement and its usefulness for TR is less well-established.<sup>40</sup>

The variable outcomes based on aetiology of secondary TR<sup>41,42</sup> as well as multiple morphologic characteristics of the valve that predict recurrence of TR following surgical TV repair,<sup>43</sup> have driven the need to redefine the classification of secondary TR based on their primary

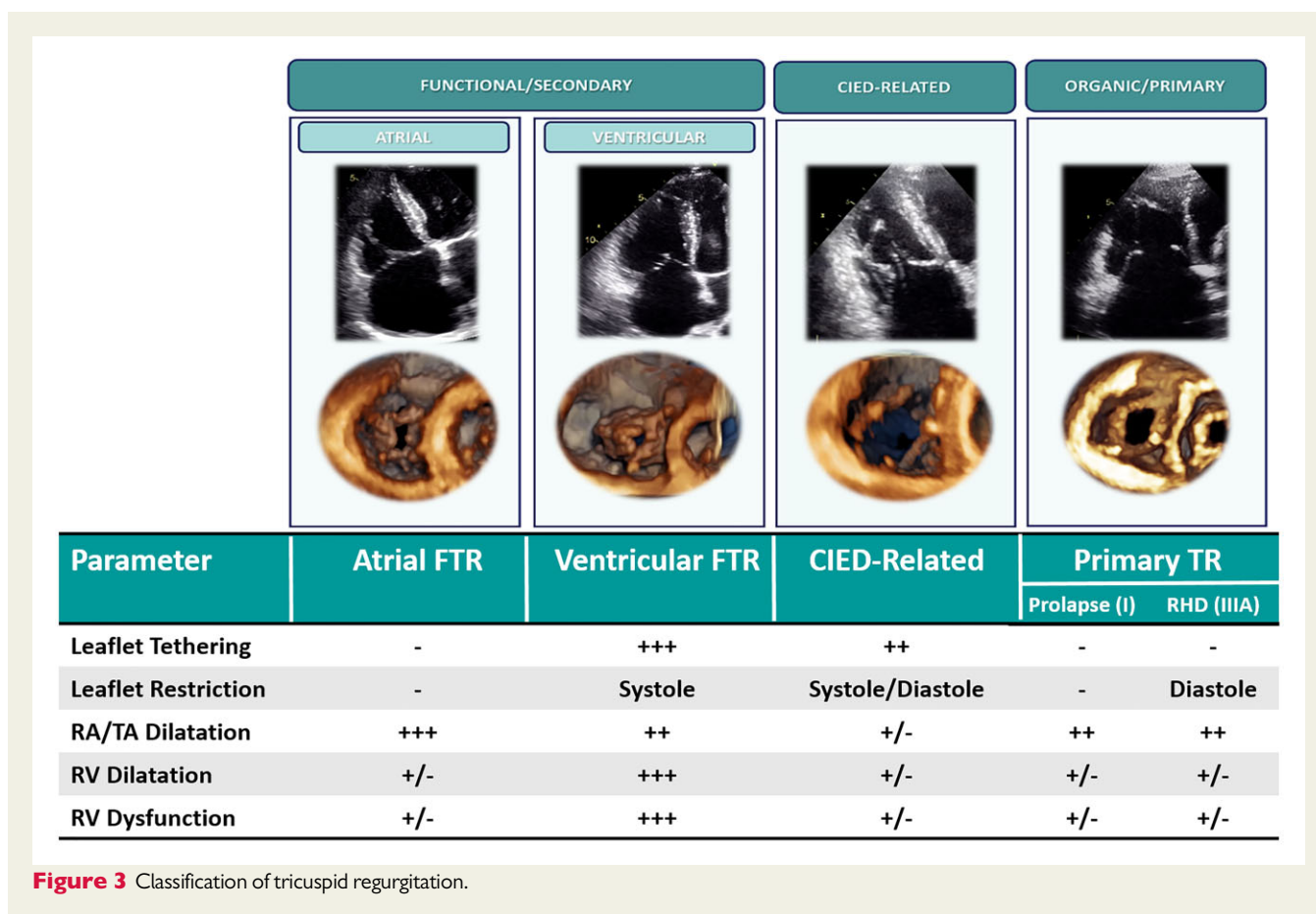


**Figure 3** Classification of tricuspid regurgitation.

cause, distinct pathophysiology and characteristic imaging features. The new classification should include differences in TV leaflet mobility and mode of coaptation, but also include characteristic differences in TA, RV, and RA remodelling and function related to the distinct pathophysiology of secondary TR, advancing the paradigm that 'not all secondary TRs are the same' (Figure 3).<sup>44</sup>

Recent prospective pathophysiologic studies using 3DE in patients with AFib have demonstrated that secondary TR develops not only as a consequence of RV remodelling, but can be caused also by TA dilation secondary to RA dilation and dysfunction in the absence of any RV abnormality, pulmonary hypertension, or left-heart disease.<sup>25,44-46</sup> This form of secondary TR (formerly known as isolated or idiopathic TR), is now commonly referred to as atrial (or atrio-genic) secondary TR and has been acknowledged in recent guidelines as a distinct entity with a fundamentally different pathophysiology with respect to the traditional form of secondary TR due to RV remodelling (referred to as ventricular secondary TR).<sup>47</sup>

Atrial secondary TR is a diagnosis of exclusion, defined by the absence of any leaflet abnormality, left ventricular (LV) dysfunction (ejection fraction <60%), left-sided valve disease, pulmonary hypertension (pulmonary artery systolic pressure >50 mmHg)<sup>47</sup> or CIED, and supported by the clinical history of the patient with evidence of longstanding or permanent AFib. From an imaging standpoint, atrial secondary TR shows greater TA enlargement and a triangular-shaped RV inflow with predominant basal dilation, as compared with

the ellipsoidal-shaped RV elongation with leaflet tethering and less TA dilation seen in patients with secondary TR caused by pulmonary hypertension or RV myocardial disease.<sup>24,26,44</sup> In one recent study, the minimal volume of RA and the TA area, but not the RV volume, determined the severity of atrial secondary TR.<sup>25</sup>

The new classification of TR discriminating the atrial from the ventricular form of secondary TR has prognostic and treatment implications.<sup>41,48,49</sup> Atrial secondary TR has a rapid progression of severity and poor outcome, and secondary RV dilation and/or dysfunction commonly develops in advanced stages. Despite limited evidence to date, rhythm control may help to decrease atrial secondary TR in some patients through reverse remodelling of RA and TA.<sup>38,46</sup> Also, this form may be particularly amenable with annuloplasty devices, because the leaflet tethering is typically minimal.<sup>44,50</sup> As longstanding ventricular secondary TR may also evolve with AFib, the diagnosis of the primary cause in advanced stages of TR can be very challenging.

## CIEDs and TR

The proportion of CIED-induced or device-mediated TR is expected to increase due to ageing of the population, increasing number of implantations, and of related complications requiring lead extraction.<sup>38,51,52</sup> Due to its multifactorial pathophysiology sharing features of both primary and secondary TR,<sup>53-55</sup> as well as different epidemiology, management and therapeutic options,

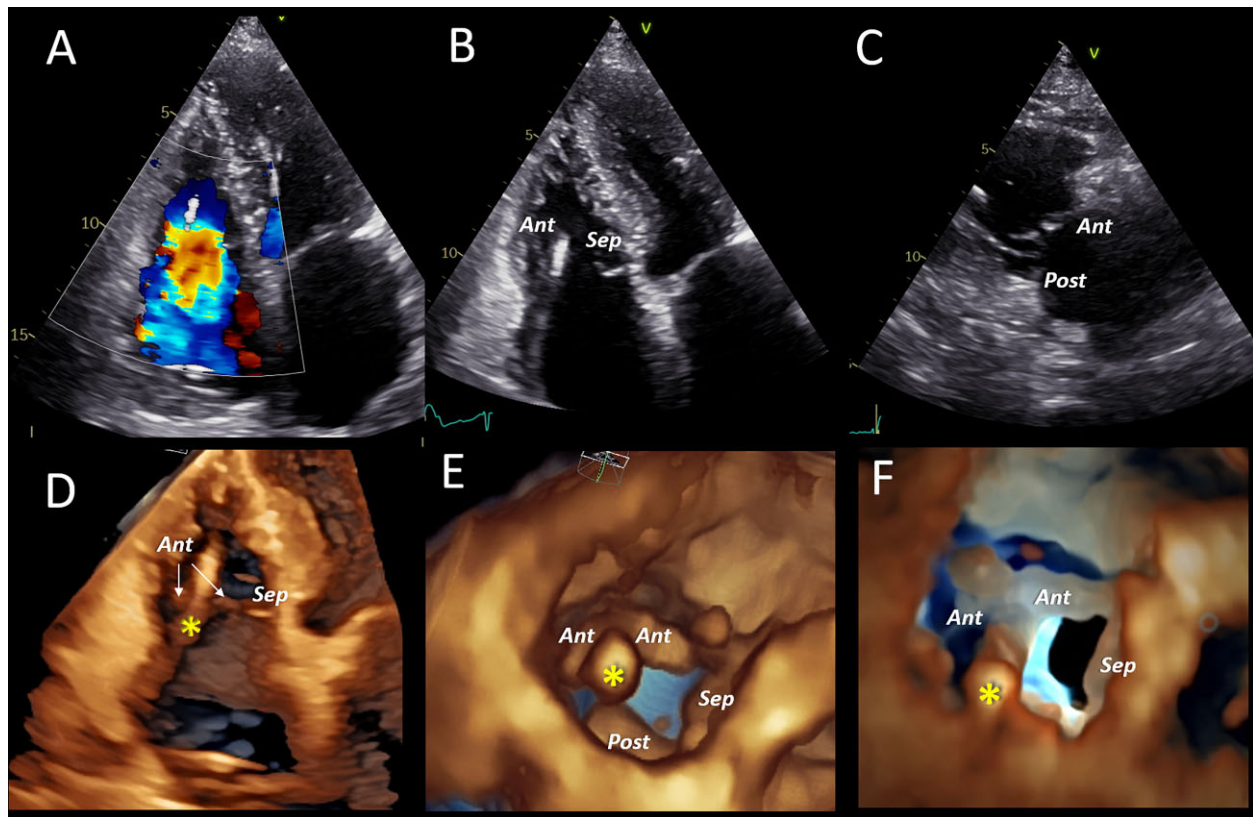


**Figure 4** Examples of cardiac implantable electronic device imaging. (A) A 4-chamber view colour Doppler image showing torrential TR in a patient with pacemaker (PM). (B) A 4-chamber view showing no apparent interference of PM catheter with anterior (Ant) and septal (Sep) leaflet, which are severely tethered and not coapting. (C) A RV inflow view showing the anterior (Ant) and posterior (Post) leaflets. The PM catheter can only be visualized at its most distal part. (D) A RV inflow 3D rendering showing a possible interference of PM catheter (asterisk) with anterior leaflet (Ant). (E) A TV 3D en face views during systole from the ventricular perspective clearly show the PM catheter (asterisk) impinging the anterior leaflet (Ant) in its mid part. (F) The same view as (E), with transillumination slightly tilted to display the close spatial relationship between PM lead (asterisk) and anterior leaflet (Ant).

it has been recently proposed to classify the CIED-related TR as a third distinct category (Figure 3).<sup>14</sup> Finally, as the presence of pacemaker lead is associated with worse outcomes with TR,<sup>56</sup> studies aimed to evaluate the results after interventional or surgical treatment should classify and address these patients as a separate category from the atrial and ventricular forms of TR.

Approximately 25–29% of patients with permanent pacemakers have TR, roughly double the prevalence in comparison groups.<sup>57</sup> However, the pathophysiological link between the presence of the device leads and either the onset of significant TR or the worsening of a pre-existing disease is a relatively recent clinical challenge. Interference of a RV transtricuspid pacing lead with the TV apparatus components might contribute to or cause TR in 7–45% of patients who received a CIED.<sup>54</sup> The large range of the incidence of significant TR after CIED implantation is likely due to the difficulty to identify the association between the presence of the wires/catheters and the dysfunction of the TV using conventional 2DE.<sup>58,59</sup> The clinical implementation of 3DE allows the documentation of this pathophysiological relationships (Figure 4, Supplementary data online, Medias S1 and S2).<sup>60</sup>

Supporting the classification of CIED-induced TR as its own category, patients with TR and a CIED can be divided in primary and secondary disease (Table 1). Primary CIED-induced TR can be defined as an increase of TR severity of  $\sim 2$  grades during follow-up after CIED implantation in patients with documented interference of the device lead with the TV apparatus. Both echocardiography and post-mortem examinations of hearts with CIED, have shown that the device leads can interfere with the TV apparatus in different ways: impinging upon a leaflet, adhering to a leaflet, interfering with the subvalvular apparatus, perforating/lacerating a leaflet, avulsion of a leaflet (which may happen during lead extraction), and transection of papillary muscles, or chordae tendineae.<sup>54</sup>

Conversely, secondary CIED-induced TR is the consequence of the remodelling of the TV following the RV dilatation due to pacing/heart failure. Seo *et al.*<sup>61</sup> reported that up to 60% of worsened TR after CIED implantation were of secondary origin. However, the two conditions can overlap since untreated primary CIED-induced TR may trigger RV dilatation due to volume overload, and leads to secondary TR. When the latter occurs, lead extraction will be ineffective to reverse TR.<sup>61,62</sup> Permanent AFib and previous open-heart

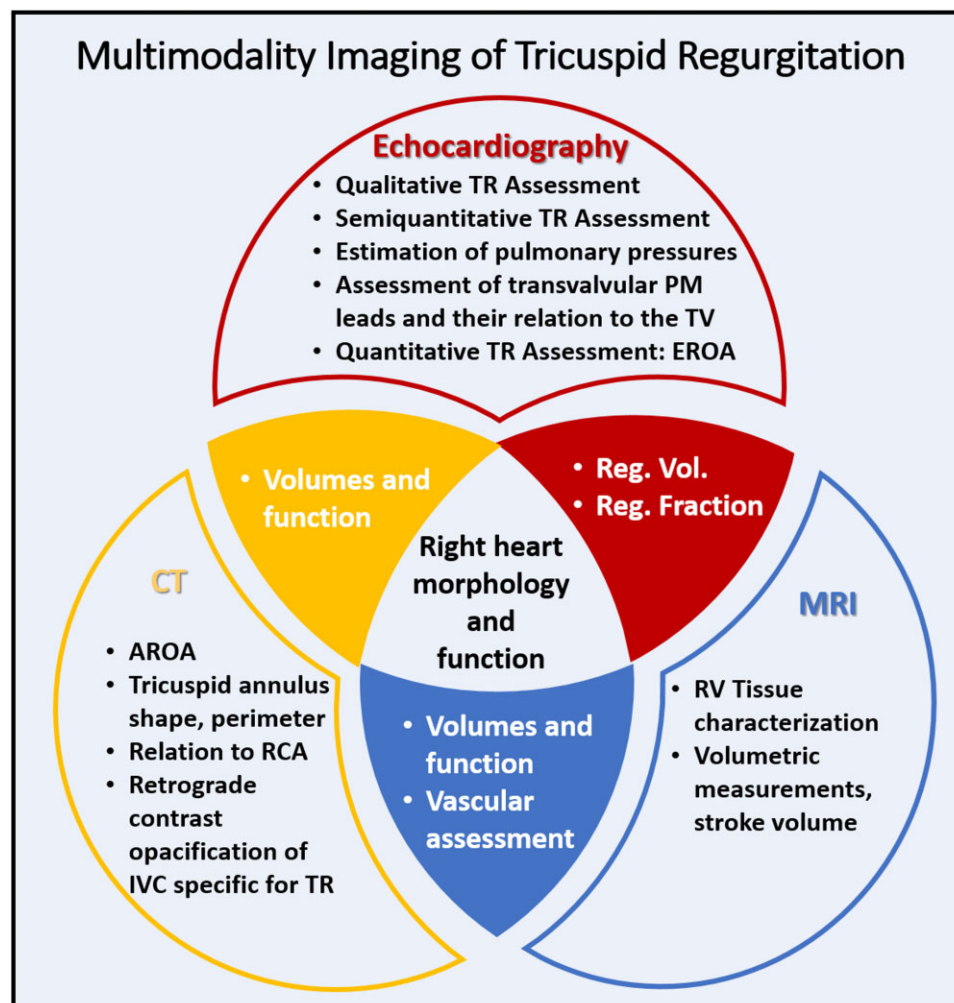


**Figure 5** Multimodality assessment of tricuspid regurgitation severity. Different imaging methods give complementary information about tricuspid regurgitation aetiology, anatomic and functional substrates as well as TR severity. AROA = anatomic regurgitant orifice, EROA = effective regurgitant orifice area, CT = computed tomography, IVC = inferior vena cava, MRI = magnetic resonance imaging, PM = pacemaker, RCA = right coronary artery, Reg. Fraction = regurgitant fraction, Reg.Vol. = regurgitant volume, RV = right ventricle, TR = tricuspid regurgitation, TV = tricuspid valve.

surgery,<sup>61</sup> as well as a pre-existing RV dilation<sup>63</sup> have been reported among the predictors of secondary CIED-induced TR.

The clinical importance of the diagnosis of CIED-induced TR is further enhanced by the fact that it affects long-term RV function<sup>64</sup> and is associated with poor outcome.<sup>57,61,64–67</sup> Accordingly, in patients in whom clinical, haemodynamic, and echocardiographic assessment provides compelling evidence of CIED-related severe TR, corrective intervention should be indicated in a timely fashion, to avoid the development of severe TA and RV dilation, and severe RV dysfunction.<sup>68</sup>

In patients with CIED-related severe TR who are considered for lead extraction, the identification of the type of lead interference by 3DE is important since the procedure can aggravate TR in patients with perforated leaflet, chordae avulsion, or in those with severe adherence or entangled leads. In a series of 200 lead extractions, increase in TR occurred in 5.6% of cases mainly in patients > 75 years, when > 2 leads were extracted and when powered sheaths were

used.<sup>69</sup> However, when the TA is dilated, the lead interference is no longer the primary problem. In a small series of patients undergoing lead extraction to manage significant TR, all patients who had TA dilatation did not benefit from lead extraction.<sup>62</sup> Patients with severe TA and/or RV dilation should be referred to surgery or transcatheter procedures. Taramasso *et al.*<sup>43</sup> analysed 470 patients with severe TR undergoing transcatheter TV repair, and compared patients with and without CIED, and reported similar rates of procedural success, residual TR, symptomatic improvement, and survival.

## Contemporary assessment of TR severity

Regardless of the imaging modality, the foundation of TR severity assessment is a thorough study of its anatomic and functional substrates. Accordingly, a detailed morphological and functional



**Table 2** Currently established and suggested (grey background) grades of tricuspid regurgitation and the respective orientation ranges for selected (semi) quantitative parameters.

Parameters	Mild	Moderate	Significant/ moderate-severe	Severe	Massive	Torrential
Vena contracta width	<3 mm	3–6.9 mm	6–6.9 mm	7–13 mm	14–20 mm	≥21 mm
EROA	20 mm <sup>2</sup>	20–29 mm <sup>2</sup>	30–39 mm <sup>2</sup>	40–59 mm <sup>2</sup>	60–79 mm <sup>2</sup>	≥80 mm <sup>2</sup>
Regurgitant volume	<15 mL	15–29 mL	30–44 mL	45–59	60–74	≥75
Regurgitant fraction 3D Echo (MRI) <sup>a</sup>	<25% (30%) <sup>a</sup>	25–44% (30–49%) <sup>a</sup>		≥45% (50%) <sup>a</sup>		
3D vena contracta				75–94 mm <sup>2</sup>	95–114 mm <sup>2</sup>	≥115 mm <sup>2</sup>

<sup>a</sup>3D Echo cutoffs from Muraru et al.<sup>76</sup> and MRI cutoffs from Zhan et al.<sup>97</sup>

characterization of the TV is advocated as a first step and described in detail above. Disease trajectories likely differ within the pathological spectrum of TR and collection and analysis of these data are indispensable components of precision medicine. Already in this initial step, imaging methods give complementary information<sup>10</sup> and careful integration and weighting according to strengths and limitations of the respective methods is advised at the beginning and throughout all steps of severity assessment. The complementary multimodality imaging approach is outlined in *Figure 5*. The recent developments of TR assessment and severity grading will be illustrate subsequently.

## Echocardiographic methods

TTE is the diagnostic imaging modality of first choice<sup>38,70</sup> and guidelines suggest grading severity should be based on qualitative, semi-quantitative, and quantitative methods.<sup>9,12,71,72</sup> In patients with significant TR, TOE can add additional aspects regarding aetiology and mechanism as well as probability of treatment strategy success. Because TR is sensitive to both pre-load and afterload, respirophasic variability as well as changes in loading conditions will introduce significant variability in TR severity. Inspiration increases pre-load and might affect the quantification. For the assessment of TR severity prior to consideration for intervention, it is recommended that the patient be in a euvoaemic state, with measurements performed during quiet respirations, and 5–10 beats averaged when the rhythm is irregular. Blood pressure and heart rate should be recorded. In addition, repeat studies may allow for a more accurate longitudinal assessment of TR severity as well as monitor the effect of TR on right heart remodelling.

### Qualitative and semi-quantitative methods

Qualitative assessment includes the assessment of structure, as well as qualitative characteristics of jet flow. Severe structural abnormalities such as a flail leaflet or marked tethering with a large coaptation gap, can be specific for severe TR (*Table 2*). Qualitative Doppler parameters include the colour flow jet characteristics (area and eccentricity), flow convergence zone, and continuous wave Doppler jet density. However, significant limitations of colour Doppler jet should be recognized. Jet flow and thus colour Doppler jet area, is governed mainly by conservation of momentum (generally defined as flow  $[Q] \times$  velocity  $[V]$ ). If  $Q = \text{EROA} \times V$ , and jet momentum  $(M) = Q \times V$ , then  $M = \text{EROA} \times V^2$ . Thus the velocity of the regurgitant jet will significantly impact the colour jet area; for the same EROA, a TR jet

with velocity of 2.5 m/s, could be a quarter of the colour jet area of a mitral regurgitant jet with a velocity of 5.0 m/s. Accordingly, colour flow imaging should only be used to diagnosing the presence of TR and a more quantitative approach is required when more than a small central TR jet is observed.<sup>12,17,37</sup>

Other qualitative and semi-quantitative measurements of TR severity also have significant pitfalls. The variable number of leaflets and commissures results in a complex jet shape and thus any evaluation relying on a single linear measurement [i.e. vena contracta (VC) diameter] may not accurately describe the complex jet. Typically, the VC is measured from the apical 4-chamber view. However, this septo-lateral dimension is frequently the minor dimension of an elliptical orifice. Some authors have recommended the use of the average VC from the parasternal inflow view and the apical 4-chamber view using a cut-off of 9 mm to differentiate moderate from severe.<sup>73,74</sup> The shape of the regurgitant orifice, and the imaging window used for measurement, thus affects the sensitivity and specificity of the VC width.

### Quantitative methods

Quantitative measurements of TR severity include the effective regurgitant orifice area (EROA), regurgitant volume (RegVol), and regurgitant fraction (RegFr). These measurements can aid treating physicians for finer risk stratification<sup>75,76</sup> and provide complementary information for interventions.<sup>77</sup>

#### PISA

The primary quantitative method recommended is the proximal isovelocity surface area (PISA) method based on the conservation of mass principle (*Figure 6*). To calculate the PISA shell area, colour Doppler baseline is shift in the direction of the regurgitant flow, the aliasing velocity ( $V_{\text{Alias}}$ ) and PISA radius ( $r$ ) can be used to calculate flow ( $2\pi r^2 \times V_{\text{Alias}}$ ). EROA is calculated by dividing the PISA flow by the peak TR velocity ( $V_{\text{TR}}$ ). EROA multiplied by TR velocity time integral ( $\text{TR}_{\text{VTI}}$ ) quantifies RegVol. Using these measurements alone, will not allow the calculation of RegFr since the total stroke volume is not measured. However, with the use of 3DE RV stroke volume, RegFr can be measured and has prognostic importance.<sup>76</sup>

Multiple limitations of the PISA methodology, should be acknowledged (*Figure 7*).<sup>78</sup> First is a problem with Doppler angle effect (*Figure 7A and B*).<sup>79,80</sup> As flow approaches a small orifice, the isovelocity shells are not actually hemispheres but have an urchinoid shape with surface

Proximal Isovelocity Surface Area	Measurements Required	Example	Calculation
Proximal Isovelocity Surface Area (PISA)	Aliasing velocity ( $V_{Alias}$ ) Color Doppler with baseline shift in the direction of regurgitant jet  Radius of PISA ( $r$ )  TR peak velocity ( $V_{TR}$ ) CW of the TR jet  TR velocity time integral ( $TR_{VTI}$ ) CW of the TR jet		<b>PISA EROA:</b> $EROA = 2\pi r^2(V_{Alias}) \div V_{TR}$ <b>TR Regurgitation Volume =</b> $EROA \times TR_{VTI}$  $EROA = (6.282 \times 0.90 \times 28\text{cm/s}) \div 180\text{cm/s}$ $= 0.88\text{cm}^2$ $Reg\ Vol = 2.01\text{cm}^2 \times 50.2\text{cm} = 100.9\text{ml}$
Quantitative Doppler	Measurements Required	Example	Calculation
2D Method	2D Diastolic TV <sub>Annular</sub> Area RV Inflow and 4Ch TV annular diameters in mid diastole  TV velocity time integral ( $TV_{VTI}$ ) PW Doppler sample volume at the annulus  TR velocity time integral ( $TR_{VTI}$ ) CW of the TR jet		<b>TV Diastolic Stroke Volume =</b> $TV_{Annular}\ Area \times TV_{VTI}$ <b>TR Regurgitation Volume =</b> $TV\ diastolic\ volume - Forward\ Stroke\ Volume$ $EROA = RegVol \div TR_{VTI}$ <b>Example:</b> <ul style="list-style-type: none"> <li>TV Diastolic SV = <math>(0.785 \times 4.3\text{cm} \times 4.5\text{cm}) \times 10.9\text{cm} = 165.6\text{ml}</math></li> <li>TR Reg Vol = 115.6ml</li> <li>EROA = <math>115.6\text{ml} \div 50.2\text{cm} = 2.30\text{cm}^2</math></li> </ul>
3D Method	Direct planimetry of the 3D Annular Area		<b>Example:</b> $3D\ Annular\ Area = 14.8\text{cm}^2$ $TV\ Diastolic\ Area = 14.8 \times 10.9\text{cm} = 161.3\text{ml}$ $TR\ Reg\ Vol = 111.3\text{ml}$ $EROA = 111.3 \div 50.2\text{cm} = 2.22\text{cm}^2$
Forward Stroke Volume used to quantify RegVol	LVOT Stroke Volume LVOT Diameter LVOT PW  Note: Forward Stroke Volume may be either the LV or RV stroke volume.		<b>Forward Stroke Volume =</b> $LVOT_{Annular}\ Area \times LVOT_{VTI}$ <b>Example:</b> $LV\ SV = (0.785 \times [2.1\text{cm}]^2) \times 14.5\text{cm} = 50.2\text{ml}$
3D Color Doppler	Measurements Required	Example	Calculation
3D Vena Contracta Area (VCA)	3D Color Doppler planimetry of the VCA  TR velocity time integral ( $TR_{VTI}$ )		$EROA \approx VCA$ <b>TR Regurgitation Volume =</b> $VCA \times TR_{VTI}$  <b>Example:</b> $3D\ VCA = 2.01\text{cm}^2$ $Reg\ Vol = 2.01\text{cm}^2 \times 50.2\text{cm} = 100.9\text{ml}$

**Figure 6** Quantitative echocardiographic methods for tricuspid regurgitation assessment. Summary of the quantitative assessment of tricuspid regurgitation (TR) by Proximal isovelocity surface area (PISA) method, volumetric Doppler quantification using both 2D and 3D methodology, and planimetry of 3D colour Doppler vena contracta area. CW, continuous wave; LV, left ventricle; LVOT, left ventricular outflow tract; PW, pulsed wave;  $r$ , radius; RegVol, regurgitant volume; RV, right ventricle;  $TR_{VTI}$ , continuous wave Doppler TR velocity time integral;  $TV_{Annulus}$ , tricuspid valve annulus;  $TV_{VTI}$ , pulsed wave Doppler annular velocity time integral;  $V_{Alias}$ , aliasing velocity; VCA, vena contracta area;  $V_{TR}$ , peak TR velocity.

area larger than a hemisphere of the same radius resulting in a 30–35% underestimation of EROA.<sup>79,80</sup> Second, similar to functional mitral regurgitation,<sup>81</sup> functional TR is temporally variable (Figure 7C and D, Supplementary data online, Media S3) and depending on the timing of PISA radius measurement, EROA may be under- or overestimated. Integrating PISA radii over the systolic time interval, improves the

estimation of functional mitral ERO,<sup>79</sup> and should be useful for TR assessment. Third, the regurgitant orifice is frequently not positioned within a planar surface (Figure 7E), thus whether the surface is funnel shaped (i.e. primary TR due to flail or marked prolapse) or the opposite wedge-shape (i.e. from marked leaflet tethering), a correction for the leaflet angle may be required. Fourth, in the

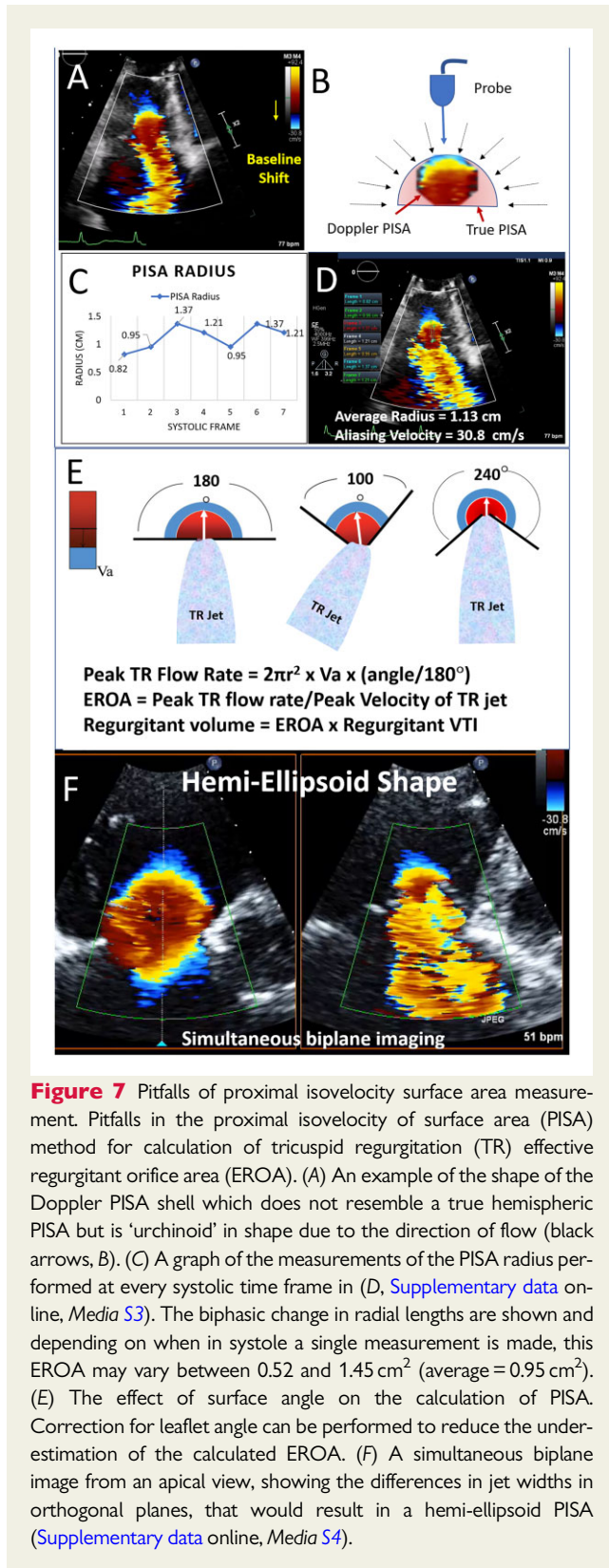


**Figure 7** Pitfalls of proximal isovelocity surface area measurement. Pitfalls in the proximal isovelocity of surface area (PISA) method for calculation of tricuspid regurgitation (TR) effective regurgitant orifice area (EROA). (A) An example of the shape of the Doppler PISA shell which does not resemble a true hemispherical PISA but is 'urchinoid' in shape due to the direction of flow (black arrows, B). (C) A graph of the measurements of the PISA radius performed at every systolic time frame in (D, [Supplementary data online, Media S3](#)). The biphasic change in radial lengths are shown and depending on when in systole a single measurement is made, this EROA may vary between 0.52 and 1.45 cm<sup>2</sup> (average = 0.95 cm<sup>2</sup>). (E) The effect of surface angle on the calculation of PISA. Correction for leaflet angle can be performed to reduce the underestimation of the calculated EROA. (F) A simultaneous biplane image from an apical view, showing the differences in jet widths in orthogonal planes, that would result in a hemi-ellipsoid PISA ([Supplementary data online, Media S4](#)).

setting of marked variability in leaflet morphology, the regurgitant orifice is often stellate or crescent-shape<sup>21</sup> and thus the PISA shell is often hemi-ellipsoid with a larger area than a

hemisphere (Figure 7F, [Supplementary data online, Media S4](#)). Finally, the low flow rates of the right heart result in a smaller difference between the PISA aliasing velocity and peak TR velocity, thus risking significant underestimation of flow by the PISA method.<sup>10</sup> Multiplying flow by  $V_{\max}/(V_{\max} - V_a)$  corrects for low flow and thus the calculation of EROA with the flow correction becomes  $2\pi r^2 (V_a)/(V_{\max} - V_a)$ .

#### Volumetric Doppler quantification

Although guidelines refer to the use of quantitative Doppler to assess TR severity, few studies have validated the methodology.<sup>6,73</sup> A refinement of the method (Figure 6) measures the TA area by: (i) measurement of orthogonal plane TA diameters in early diastole (typically inflow and 4-chamber views) using an ellipse formula, or (ii) 3D planimetry of the TA area.<sup>6</sup> Diastolic stroke volume is quantified by multiplying TA area by the TV inflow VTI ( $TV_{VTI}$ ) obtained by placing the pulse-wave sample volume at the level of diastolic annular plane. The forward systolic stroke volume (either from the RV or LV outflow tract) is subtracted from the diastolic stroke volume resulting in a measurement of RegVol. Dividing RegVol by  $TR_{VTI}$  calculates the EROA, and dividing RegVol by RV stroke volume calculates RegFr. The main limitations of the method rely on the geometric assumptions about the shape of the TA and the need of no significant concomitant regurgitation of the pulmonary and/or aortic and mitral valves.

#### 3D colour Doppler quantification

Several studies have shown the feasibility of 3D colour Doppler planimetry of the VC area (VCA) by both TTE<sup>73</sup> and TOE (Figure 6).<sup>82</sup> Studies suggest the quantitative cut-offs for severe TR are: 3D-VCA  $\geq 0.60$ – $0.61$  cm<sup>2</sup>,<sup>73,82</sup> Doppler-EROA  $\geq 0.65$  cm<sup>2</sup>, and PISA-EROA  $\geq 0.34$  cm<sup>2</sup>.<sup>73</sup> The 3D-VCA method correlates well with quantitative Doppler method ( $r = 0.92$ ;  $P < 0.0001$ ). However, the PISA EROA significantly underestimates these other methods, likely due to the pitfalls previously described. The moderate correlation between 3D-VCA and PISA-EROA methods ( $r = 0.60$ ;  $P = 0.01$ ) is improved in more circular orifices ( $r = 0.87$ ;  $P = 0.001$ ).<sup>73</sup>

#### Other relevant echocardiographic parameters

Multiple guidelines have suggested that systolic reversal of hepatic vein flow is a sign of severe TR.<sup>8,9</sup> The guidelines also clearly state that this sign is non-specific and is influenced by many other factors (RV diastolic function, atrial fibrillation, RA pressure, or compliance).<sup>83</sup> Moreover, in the original reports systolic flow reversal in the hepatic vein was a sign of moderate or severe TR.<sup>83,84</sup> Hepatic vein systolic flow reversal may be seen in patients with moderate TR, particularly in the setting of high RA or RV pressures for other reasons, and it should not be used as a sole specific criteria for severe TR, but rather as supportive evidence for clinically important disease. In patients with significant TR, RV remodelling due to both dilatation and dysfunction should be assessed. Basal and mid ventricular RV septo-lateral dimensions as well as apex to TA length, are measured from an RV focused view, which typically yields larger dimensions than the apical 4-chamber or RV modified views.<sup>85,86</sup> RV function can be assessed by TA plane systolic excursion, tissue-Doppler systolic velocity, fractional area change, and RV-free wall or global

longitudinal strain. Measurements of RV function have important prognostic value in patients with TR.<sup>26,87,88</sup> Multiple linear dimension measurements can be used to describe RV size however 3D TTE compares favourably with CMR for quantitation of volumes<sup>89</sup> and can be used to quantify RV and RA volumes, as well as TV tenting volume and TA area.<sup>44</sup> Indexing RV contractility to after-load, or RV–pulmonary artery (PA) coupling, describes a normal physiologic state where mechanical stroke work is transferred efficiently to the pulmonary circuit and RV contractility can increase when after-load increases. A recent study in patients with severe secondary TR showed RV–PA coupling using echocardiographic measures, was independently associated with all-cause mortality.<sup>90</sup> Doppler estimates of PA pressure may underestimate invasive measurements, particularly in the setting of greater TR severity, worse LV and RV function and the V-wave cut-off sign on spectral Doppler.<sup>91</sup>

### Grading of TR severity

Two areas of the TR severity spectrum have been specific areas of interest in recent years, owing to the development of low-risk transcatheter repair strategies: First is the transition zone where the TR volume overload exceeds the individual compensatory reserve and results in heart failure, cardiovascular morbidity, and mortality.<sup>75,76,92,93</sup> This is of specific interest as there might be stages exceeding the adaptive potential with consequent irreversible failure. In this group, progression of TR is often accelerated due to biatrial and annular dilatation<sup>52,94</sup> and appears to be clinically important for planning of close follow-ups. Selected studies that focused on these aspects are listed in *Table 2*. Second, is the extreme end of the TR spectrum grouped under the umbrella term ‘severe’ seems to be far more heterogeneous than for mitral regurgitation with EROAs >80 mm<sup>2</sup>.<sup>11,42,74,95,96</sup> Post-interventional reduction of such exuberant TR grades might be clinically relevant but still severe, therefore one term for this heterogeneous group might not reflect profound reductions achieved by transcatheter treatments. Selected studies on the expanded grading are listed in *Table 2*.

### Cardiac magnetic resonance assessment

Cardiac magnetic resonance imaging (CMR) has the advantage of high spatial resolution and excellent endocardial border delineation. These aspects are specifically valuable for the assessment of complex RV structure and function. TR can be qualitatively assessed by the signal drop (spin, dephasing) that occurs within areas of non-laminar flow/areas of flow acceleration.<sup>10</sup> Due to only modest correlation with quantitative assessment, grading TR severity by qualitative assessment is limited. From a technical perspective, CMR is an optimal method for quantitating TR. One advantage is that the reference stroke volume can be calculated reliably from three different methods (phase contrast imaging from the pulmonic valve or aortic valve, and volumetric LV stroke volume). A recent study has demonstrated the prognostic value of the RegVol and fraction by CMR regarding subsequent mortality in an all-comer cohort.<sup>97</sup> More validation and differences in specific patient cohorts will be mandatory to strengthen the role

of CMR TR quantification in clinical practice. Another important feature of CMR is tissue characterization.<sup>98</sup> Late gadolinium enhancement and more recently T1 mapping as well as extracellular volume quantitation can provide information about myocardial impairment and fibrotic remodelling. Limitations of CMR include the presence of arrhythmias and transvalvular pacemaker leads often present in patients with TR. Intra- and inter-rater reproducibility was demonstrated to be adequate for CMR assessed RegVol and RegFr.<sup>97</sup> There is satisfactory accuracy between echocardiographic and CMR for TR quantification but often a deviation by 1° of severity.<sup>99</sup>

### Computed tomography

Cardiac CT provides complementary information and will likely become crucial for planning structural interventions. Assessment of the TA shape, perimeter and diameters, and localization of the right coronary artery and its course within the atrioventricular groove as well as its distance from the TA are specific strengths of CT imaging.<sup>10,92</sup>

## Treatment options for functional TR: should anatomy guide us?

The choice among the different surgical and interventional options available to treat TR<sup>43,100,101</sup> should be driven by the underlying mechanism of regurgitation, by the patient conditions, and the aetiology of the disease. The anatomic-functional assessment of the TV becomes of primary importance to choose between replacement and repair. In patients with anatomy suitable for repair, the fine details of anatomy and function of the valve components can influence the repair strategy and the techniques used.

Multimodality imaging is used to select the best treatment strategy.<sup>102,103</sup> In the era of catheter-based technologies, device selection supported by the analysis of the anatomical features is critical to obtain the best results. The assessment of the mechanism of regurgitation should include annular, leaflet, and subannular components.<sup>92</sup> Valve dysfunction can be classified similarly to the Carpentier functional classification used for the mitral regurgitation to use a standardized communication approach.<sup>104</sup>

In the case of functional TR, the main components of valve regurgitation are annular dilatation and leaflet tethering.<sup>92</sup> According to the prevalent mechanism, one or more corrective actions are used to re-establish valve competence. Valve replacement is preferred for patients in whom the dysfunction and/or the geometrical distortion of the apparatus is more advanced and valve repair is predicted to be inefficient or not durable.

In low-risk patients, surgery remains the gold standard treatment of functional TR.<sup>38,47</sup> In a recent study in which a dedicated risk score model was developed to predict the outcome of patients after ITVS for severe TR using eight parameters: age ≥70 years (1 point), New York Heart Association Class III–IV (1 point), right-sided heart failure signs (2 points), daily dose of furosemide ≥125 mg (2 points), glomerular filtration rate <30 mL/min (2 points), elevated bilirubin (2



failure in case of leaflet tethering and RV dysfunction/remodelling.<sup>106</sup> In this case, additional leaflet procedures (such as leaflet augmentation or the clover technique) are used to improve short- and long-term durability.<sup>107,108</sup> Repair of complex congenital anomalies (e.g. Ebstein anomaly), or endocarditic TR is only possible with a surgical approach.<sup>109,110</sup> In patients with functional TR and advanced disease undergoing surgery, there is a recent trend for a low threshold to valve replacement as opposed to repair. Given the high-risk profile of reinterventions, a definitive solution is often preferred although the new interventional algorithms may influence the choice in the future.<sup>111</sup> There are no anatomical limits to surgical TV replacement, therefore imaging plays a minimal role in guiding the prosthesis selection and the surgical technique of implantation.

Imaging remains the cornerstone of all decisions related to interventional procedures, particularly in case of repair.<sup>112</sup> In most cases, the intervention targets the culprit lesion with a single device acting on a single dysfunctional element, as compared with surgery in which combined procedures are common. In the last decade, a large number of devices have been introduced to mimic any surgical procedure via a catheter. Most procedures are still investigational, while some interventional approaches are becoming very common. The largest experience is related to the transcatheter edge-to-edge repair (TEER).<sup>113</sup> Most patients can be treated using the TEER approach, however, early data show that there are patient populations whose anatomy or pathophysiology may not result in either optimal reduction to  $\leq 2+$  TR, or improved outcomes (Table 3).<sup>22,23,77,114–118</sup> Procedural success of tricuspid TEER, typically defined as successful clip placement and reduction of TR  $\geq 1$  grade on TTE at 30 days, was the only predictor for freedom from clinical outcomes and independently predicted freedom from the combined endpoint. On multivariate analysis, a smaller TV coaptation gap ( $<7.2$  mm) and a central/anteroseptal TR jet location independently predicted transcatheter TR repair success.<sup>114</sup> Using the newer generation of devices with longer device arms, coaptation gaps of up to 8.4 mm may be achievable.<sup>77</sup> Multiple studies have suggested that patients with massive or torrential disease, also have worse procedural success and outcomes with a VC width  $\geq 14$  mm<sup>42,119</sup> or an effective regurgitation orifice area by PISA method<sup>115,120</sup> of  $>60$ – $70$  mm<sup>2</sup> were associated with lower procedural success. Tricuspid TEER success has also recently been associated with valve morphology; the more complex the morphology, the lower the procedural success<sup>22</sup> which may then affect overall outcomes.<sup>23</sup> Outcomes following tricuspid TEER have been strongly correlated with RV ejection fraction.<sup>117,118</sup> Remodelling of the RV has been seen in patients following tricuspid TEER<sup>120</sup>; however, the extent of remodelling and relationship to baseline measures is currently unknown.

Some annuloplasty devices are available and could be used as stand-alone procedure in patients in whom leaflet tethering is less pronounced. The main factors related to procedural success are the size of the TA, the absence of leaflet restricted motion, and the distance of the TA from the right coronary artery (assessed by CT scan). In theory, annuloplasty and TEER could be used in combination similar to the surgical approach of annuloplasty and clover technique. In patients with more advanced geometrical changes of the TV components and of the RV, valve replacement is an option still in its early phase, with no devices available for commercial use. Patient selection is mainly based on CT scan to assess annular dimensions, anatomy

and size of the RV, and the position of the vena cava. Echocardiography and right heart catheterization are fundamental for patient selection to rule out patients with too advanced right heart disease and significantly increased pulmonary resistance, both of which may be integral to risk stratification.<sup>10,38</sup>

## Conclusion

The independent association of mortality with severity of untreated TR, along with a high mortality associated with isolated TR surgery, has led to intense interest surrounding the improvement in characterization, diagnosis, and treatment of TR. The new classification systems for TR aetiology and severity presented in this review, have anatomic and clinical relevance. The issues surrounding the accurate non-invasive quantitative assessment of TR may be addressed by the use of advanced imaging methods and techniques. Finally, patient-specific transcatheter therapies will undoubtedly require the use of morphologic and TR severity parameters for appropriate device choice.

## Supplementary data

Supplementary data are available at *European Heart Journal - Cardiovascular Imaging* online.

**Conflict of interest:** R.T.H. reports speaker fees from Abbott Vascular, Baylis Medical, Edwards Lifescience; institutional consulting agreement without direct compensation with Abbott Vascular, Boston Scientific, Edwards Lifescience, Medtronic; Equity with Navigate.

## Data availability

No new data were generated or analysed in support of this review.

## References

- Chorin E, Rozenbaum Z, Topilsky Y, Konigstein M, Ziv-Baran T, Richert E et al. Tricuspid regurgitation and long-term clinical outcomes. *Eur Heart J Cardiovasc Imaging* 2020;**21**:157–65.
- Benfari G, Antoine C, Miller WL, Thapa P, Topilsky Y, Rossi A et al. Excess mortality associated with functional tricuspid regurgitation complicating heart failure with reduced ejection fraction. *Circulation* 2019;**140**:196–206.
- Enriquez-Sarano M, Messika-Zeitoun D, Topilsky Y, Tribouilloy C, Benfari G, Michelena H. Tricuspid regurgitation is a public health crisis. *Prog Cardiovasc Dis* 2019;**62**:447–51.
- Zack CJ, Fender EA, Chandrashekar P, Reddy YNV, Bennett CE, Stulak JM et al. National trends and outcomes in isolated tricuspid valve surgery. *J Am Coll Cardiol* 2017;**70**:2953–60.
- Dreyfus J, Flagiello M, Bazire B, Eggenspieler F, Viau F, Riant E et al. Isolated tricuspid valve surgery: impact of aetiology and clinical presentation on outcomes. *Eur Heart J* 2020;**41**:4304–17.
- Hahn RT, Meduri CU, Davidson CJ, Lim S, Nazif TM, Ricciardi MJ et al. Early feasibility study of a transcatheter tricuspid valve annuloplasty: SCOUT trial 30-day results. *J Am Coll Cardiol* 2017;**69**:1795–806.
- Navia JL, Kapadia S, Elgharably H, Harb SC, Krishnaswamy A, Unai S et al. First-in-human implantations of the navigate bioprosthesis in a severely dilated tricuspid annulus and in a failed tricuspid annuloplasty ring. *Circ Cardiovasc Interv* 2017;**10**:e005840.
- Zoghbi WA, Adams D, Bonow RO, Enriquez-Sarano M, Foster E, Grayburn PA et al. Recommendations for noninvasive evaluation of native valvular regurgitation: a report from the American Society of Echocardiography Developed in Collaboration with the Society for Cardiovascular Magnetic Resonance. *J Am Soc Echocardiogr* 2017;**30**:303–71.

9. Lancellotti P, Moura L, Pierard LA, Agricola E, Popescu BA, Tribouilloy C *et al.*: European Association of Echocardiography. European Association of Echocardiography recommendations for the assessment of valvular regurgitation. Part 2: mitral and tricuspid regurgitation (native valve disease). *Eur J Echocardiogr* 2010;**11**:307–32.
10. Hahn RT, Thomas JD, Khalique OK, Cavalante JL, Praz F, Zoghbi WA. Imaging assessment of tricuspid regurgitation severity. *JACC Cardiovasc Imaging* 2019;**12**:469–90.
11. Hahn RT, Zamorano JL. The need for a new tricuspid regurgitation grading scheme. *Eur Heart J Cardiovasc Imaging* 2017;**18**:1342–3.
12. Zaidi A, Oxborough D, Augustine DX, Bedair R, Harkness A, Rana B *et al.* Echocardiographic assessment of the tricuspid and pulmonary valves: a practical guideline from the British Society of Echocardiography. *Echo Res Pract* 2020;**7**:G95–122.
13. Anderson RH, Loukas M. The importance of attitudinally appropriate description of cardiac anatomy. *Clin Anat* 2009;**22**:47–51.
14. Praz F, Muraru D, Kreidel F, Lurz P, Hahn RT, Delgado V *et al.* Transcatheter treatment for tricuspid valve disease. *EuroIntervention* 2021;**17**:791–808.
15. Silver MD, Lam JH, Ranganathan N, Wigle ED. Morphology of the human tricuspid valve. *Circulation* 1971;**43**:333–48.
16. Tretter JT, Sarwark AE, Anderson RH, Spicer DE. Assessment of the anatomical variation to be found in the normal tricuspid valve. *Clin Anat* 2016;**29**:399–407.
17. Hahn RT. State-of-the-art review of echocardiographic imaging in the evaluation and treatment of functional tricuspid regurgitation. *Circ Cardiovasc Imaging* 2016;**9**:e005332.
18. Xanthos T, Dalivigkas I, Ekmektzoglou KA. Anatomic variations of the cardiac valves and papillary muscles of the right heart. *Ital J Anat Embryol* 2011;**116**:111–26.
19. Wafae N, Hayashi H, Gerola LR, Vieira MC. Anatomical study of the human tricuspid valve. *Surg Radiol Anat* 1990;**12**:37–41.
20. Holda MK, Zhingre Sanchez JD, Bateman MG, Iazzo PA. Right atrioventricular valve leaflet morphology redefined. *JACC Cardiovasc Interv* 2019;**12**:169–78.
21. Hahn RT, Weckbach LT, Noack T, Hamid N, Kitamura M, Bae R *et al.* Proposal for a standard echocardiographic tricuspid valve nomenclature. *JACC Cardiovasc Imaging* 2021;**14**:1299–305.
22. Kitamura M, Kresoja KP, Besler C, Leontyev S, Kiefer P, Rommel KP *et al.* Impact of tricuspid valve morphology on clinical outcomes after transcatheter edge-to-edge repair. *JACC Cardiovasc Interv* 2021;**14**:1616–8.
23. Sugiura A, Tanaka T, Kavsur R, Öztürk C, Vogelhuber J, Wilde N *et al.* Leaflet configuration and residual tricuspid regurgitation after transcatheter edge-to-edge tricuspid repair. *JACC Cardiovasc Interv* 2021;**14**:2260–70.
24. Muraru D, Guta AC, Ochoa-Jimenez RC, Bartos D, Aruta P, Mihaila S *et al.* Functional regurgitation of atrioventricular valves and atrial fibrillation: an elusive pathophysiological link deserving further attention. *J Am Soc Echocardiogr* 2020;**33**:42–53.
25. Guta AC, Badano LP, Tomaselli M, Mihalcea D, Bartos D, Parati G *et al.* The pathophysiological link between right atrial remodeling and functional tricuspid regurgitation in patients with atrial fibrillation: a three-dimensional echocardiography study. *J Am Soc Echocardiogr* 2021;**34**:585–94.e1.
26. Florescu DR, Muraru D, Florescu C, Volpato V, Caravita S, Perger E *et al.* Right heart chambers geometry and function in patients with the atrial and the ventricular phenotypes of functional tricuspid regurgitation. *Eur Heart J Cardiovasc Imaging* 2022;**23**:930–940.
27. Utsunomiya H, Itabashi Y, Kobayashi S, Rader F, Siegel RJ, Shiota T. Clinical impact of size, shape, and orientation of the tricuspid annulus in tricuspid regurgitation as assessed by three-dimensional echocardiography. *J Am Soc Echocardiogr* 2020;**33**:191–200 e1.
28. Otto AC, Velichkov M, Hamadanchi A, Schulze PC, Moebius-Winkler S. The impact of tricuspid annular geometry on outcome after percutaneous edge-to-edge repair for severe tricuspid regurgitation. *Cardiol J* 2021;**28**:579–88.
29. Muraru D, Bidviene J, Cavalli G, Cavaliere A, Badano LP. Tricuspid regurgitation in a patient with ascending aorta aneurysm. *Eur Heart J Cardiovasc Imaging* 2016;**17**:1435.
30. Prihadi EA, Delgado V, Leon MB, Enriquez-Sarano M, Topilsky Y, Bax JJ. Morphologic types of tricuspid regurgitation: characteristics and prognostic implications. *JACC Cardiovasc Imaging* 2019;**12**:491–9.
31. van Rosendaal PJ, Kamperidis V, Kong WK, van Rosendaal AR, van der Kley F, Ajmone Marsan N *et al.* Computed tomography for planning transcatheter tricuspid valve therapy. *Eur Heart J* 2017;**38**:665–74.
32. Addetia K, Muraru D, Veronesi F, Jenei C, Cavalli G, Besser SA *et al.* 3-dimensional echocardiographic analysis of the tricuspid annulus provides new insights into tricuspid valve geometry and dynamics. *JACC Cardiovasc Imaging* 2019;**12**:401–12.
33. Ton-Nu TT, Levine RA, Handschumacher MD, Dorer DJ, Yosefy C, Fan D *et al.* Geometric determinants of functional tricuspid regurgitation: insights from 3-dimensional echocardiography. *Circulation* 2006;**114**:143–9.
34. Hirasawa K, Fortuni F, van Rosendaal PJ, Ajmone Marsan N, Bax JJ, Delgado V. Association between computed tomography-derived tricuspid annular dimensions and prognosis: insights from whole-beat computed tomography assessment. *Eur Heart J Cardiovasc Imaging* 2021;jeab133. doi: 10.1093/ehjci/jeab133.
35. Topilsky Y, Maltais S, Medina Inojosa J, Oguz D, Michelena H, Maalouf J *et al.* Burden of tricuspid regurgitation in patients diagnosed in the community setting. *JACC Cardiovasc Imaging* 2019;**12**:433–42.
36. Min SY, Song JM, Kim JH, Jang MK, Kim YJ, Song H *et al.* Geometric changes after tricuspid annuloplasty and predictors of residual tricuspid regurgitation: a real-time three-dimensional echocardiography study. *Eur Heart J* 2010;**31**:2871–80.
37. Muraru D, Hahn RT, Soliman OI, Faletra FF, Basso C, Badano LP. 3-dimensional echocardiography in imaging the tricuspid valve. *JACC Cardiovasc Imaging* 2019;**12**:500–15.
38. Vahanian A, Beyersdorf F, Praz F, Milojevic M, Baldus S, Bauersachs J *et al.* 2021 ESC/EACTS guidelines for the management of valvular heart disease. *Eur Heart J* 2021;ehab395. doi: 10.1093/eurheartj/ehab395.
39. Naser JA, Kucuk HO, Ciobanu AO, Jouni H, Oguz D, Thaden JJ *et al.* Atrial fibrillation is associated with large beat-to-beat variability in mitral and tricuspid annulus dimensions. *Eur Heart J Cardiovasc Imaging* 2021;**22**:1362–1373.
40. Antunes MJ, Rodriguez-Palomares J, Prendergast B, De Bonis M, Rosenhek R, Al-Attar N *et al.*; on behalf of the ESC Working Groups of Cardiovascular Surgery and Valvular Heart Disease. Management of tricuspid valve regurgitation: position statement of the European Society of Cardiology Working Groups of Cardiovascular Surgery and Valvular Heart Disease. *Eur J Cardiothorac Surg* 2017;**52**:1022–30.
41. Topilsky Y, Nkomo VT, Vatury O, Michelena HI, Letourneau T, Suri RM *et al.* Clinical outcome of isolated tricuspid regurgitation. *JACC Cardiovasc Imaging* 2014;**7**:1185–94.
42. Santoro C, Marco Del Castillo A, Gonzalez-Gomez A, Monteagudo JM, Hinojar R, Lorente A *et al.* Mid-term outcome of severe tricuspid regurgitation: are there any differences according to mechanism and severity? *Eur Heart J Cardiovasc Imaging* 2019;**20**:1035–42.
43. Taramasso M, Gavazzoni M, Pozzoli A, Dreyfus GD, Bolling SF, George I *et al.* Tricuspid regurgitation: predicting the need for intervention, procedural success, and recurrence of disease. *JACC Cardiovasc Imaging* 2019;**12**:605–21.
44. Muraru D, Addetia K, Guta AC, Ochoa-Jimenez RC, Genovese D, Veronesi F *et al.* Right atrial volume is a major determinant of tricuspid annulus area in functional tricuspid regurgitation: a three-dimensional echocardiographic study. *Eur Heart J Cardiovasc Imaging* 2021;**22**:660–9.
45. Ortiz-Leon XA, Posada-Martinez EL, Trejo-Paredes MC, Ivey-Miranda JB, Pereira J, Crandall I *et al.* Understanding tricuspid valve remodeling in atrial fibrillation using three-dimensional echocardiography. *Eur Heart J Cardiovasc Imaging* 2020;**21**:747–55.
46. Muraru D, Caravita S, Guta AC, Mihalcea D, Branzi G, Parati G *et al.* Functional tricuspid regurgitation and atrial fibrillation: which comes first, the chicken or the egg? *Case* 2020;**4**:458–63.
47. Otto CM, Nishimura RA, Bonow RO, Carabello BA, Erwin JP 3rd, Gentile F *et al.* 2020 ACC/AHA guideline for the management of patients with valvular heart disease: executive summary: a report of the American College of Cardiology/American Heart Association Joint Committee on Clinical Practice Guidelines. *J Am Coll Cardiol* 2021;**77**:450–500.
48. Chen E, L'Official G, Guerin A, Dreyfus J, Lavie-Badie Y, Sportouch C *et al.* Natural history of functional tricuspid regurgitation: impact of cardiac output. *Eur Heart J Cardiovasc Imaging* 2021;**22**:878–85.
49. Hell MM, Emrich T, Kreidel F, Kreitner KF, Schoepf UJ, Munzel T *et al.* Computed tomography imaging needs for novel transcatheter tricuspid valve repair and replacement therapies. *Eur Heart J Cardiovasc Imaging* 2021;**22**:601–10.
50. Badano LP, Caravita S, Rella V, Guida V, Parati G, Muraru D. The added value of 3-dimensional echocardiography to understand the pathophysiology of functional tricuspid regurgitation. *JACC Cardiovasc Imaging* 2021;**14**:683–9.
51. Anvardeen K, Rao R, Hazra S, Hay K, Dai H, Stoyanov N *et al.* Prevalence and significance of tricuspid regurgitation post-endocardial lead placement. *JACC Cardiovasc Imaging* 2019;**12**:562–4.
52. Prihadi EA, van der Bijl P, Gursoy E, Abou R, Mara Vollema E, Hahn RT *et al.* Development of significant tricuspid regurgitation over time and prognostic implications: new insights into natural history. *Eur Heart J* 2018;**39**:3574–81.
53. Polewczyk A, Kutarski A, Tomaszewski A, Brzozowski W, Czajkowski M, Polewczyk M *et al.* Lead dependent tricuspid dysfunction: analysis of the mechanism and management in patients referred for transvenous lead extraction. *Cardiol J* 2013;**20**:402–10.
54. Addetia K, Harb SC, Hahn RT, Kapadia S, Lang RM. Cardiac implantable electronic device lead-induced tricuspid regurgitation. *JACC Cardiovasc Imaging* 2019;**12**:622–36.

55. Vaturi M, Kusniec J, Shapira Y, Nevzorov R, Yedidya I, Weisenberg D et al. Right ventricular pacing increases tricuspid regurgitation grade regardless of the mechanical interference to the valve by the electrode. *Eur J Echocardiogr* 2010; **11**:550–3.
56. Prihadi EA, van der Bijl P, Gursoy E, Abou R, Mara Vollema E, Hahn RT et al. Development of significant tricuspid regurgitation over time and prognostic implications: new insights into natural history. *Eur Heart J* 2018; **39**:3574–81.
57. Al-Bawardy R, Krishnaswamy A, Bhargava M, Dunn J, Wazni O, Tuzcu EM et al. Tricuspid regurgitation in patients with pacemakers and implantable cardiac defibrillators: a comprehensive review. *Clin Cardiol* 2013; **36**:249–54.
58. Seo Y, Ishizu T, Nakajima H, Sekiguchi Y, Watanabe S, Aonuma K. Clinical utility of 3-dimensional echocardiography in the evaluation of tricuspid regurgitation caused by pacemaker leads. *Circ J* 2008; **72**:1465–70.
59. Lin G, Nishimura RA, Connolly HM, Dearani JA, Sundt TM 3rd, Hayes DL. Severe symptomatic tricuspid valve regurgitation due to permanent pacemaker or implantable cardioverter-defibrillator leads. *J Am Coll Cardiol* 2005; **45**:1672–5.
60. Addetia K, Maffessanti F, Mediratta A, Yamat M, Weinert L, Moss JD et al. Impact of implantable transvenous device lead location on severity of tricuspid regurgitation. *J Am Soc Echocardiogr* 2014; **27**:1164–75.
61. Seo J, Kim DY, Cho I, Hong GR, Ha JW, Shim CY. Prevalence, predictors, and prognosis of tricuspid regurgitation following permanent pacemaker implantation. *PLoS One* 2020; **15**:e0235230.
62. Nazmul MN, Cha YM, Lin G, Asirvatham SJ, Powell BD. Percutaneous pacemaker or implantable cardioverter-defibrillator lead removal in an attempt to improve symptomatic tricuspid regurgitation. *Europace* 2013; **15**:409–13.
63. Riesenhuber M, Spannbauser A, Gwechenberger M, Pezawas T, Schukro C, Stix G et al. Pacemaker lead-associated tricuspid regurgitation in patients with or without pre-existing right ventricular dilatation. *Clin Res Cardiol* 2021; **110**: 884–94.
64. Papageorgiou N, Falconer D, Wyeth N, Lloyd G, Pellerin D, Speechly-Dick E et al. Effect of tricuspid regurgitation and right ventricular dysfunction on long-term mortality in patients undergoing cardiac devices implantation: >10-year follow-up study. *Int J Cardiol* 2020; **319**:52–6.
65. Arabi P, Özer N, Ateş AH, Yorgun H, Oto A, Aytemir K. Effects of pacemaker and implantable cardioverter defibrillator electrodes on tricuspid regurgitation and right sided heart functions. *Cardiol J* 2015; **22**:637–44.
66. Delling FN, Hassan ZK, Piatkowski G, Tsao CW, Rajabali A, Markson LJ et al. Tricuspid regurgitation and mortality in patients with transvenous permanent pacemaker leads. *Am J Cardiol* 2016; **117**:988–92.
67. Hoke U, Auger D, Thijssen J, Wolterbeek R, van der Velde ET, Holman ER et al. Significant lead-induced tricuspid regurgitation is associated with poor prognosis at long-term follow-up. *Heart* 2014; **100**:960–8.
68. Chang JD, Manning WJ, Ebrille E, Zimetbaum PJ. Tricuspid valve dysfunction following pacemaker or cardioverter-defibrillator implantation. *J Am Coll Cardiol* 2017; **69**:2331–41.
69. Coffey JO, Sager SJ, Gangireddy S, Levine A, Viles-Gonzalez JF, Fischer A. The impact of transvenous lead extraction on tricuspid valve function. *Pacing Clin Electrophysiol* 2014; **37**:19–24.
70. Otto CM, Nishimura RA, Bonow RO, Carabello BA, Erwin JP, Gentile F et al. 2020 ACC/AHA guideline for the management of patients with valvular heart disease: a report of the American College of Cardiology/American Heart Association Joint Committee on Clinical Practice Guidelines. *Circulation* 2021; **143**:e72–227.
71. Lancellotti P, Tribouilloy C, Hagendorff A, Popescu BA, Edvardsen T, Pierard LA et al; Scientific Document Committee of the European Association of Cardiovascular Imaging. Recommendations for the echocardiographic assessment of native valvular regurgitation: an executive summary from the European Association of Cardiovascular Imaging. *Eur Heart J Cardiovasc Imaging* 2013; **14**: 611–44.
72. Zoghbi WA, Asch FM, Bruce C, Gillam LD, Grayburn PA, Hahn RT et al. Guidelines for the evaluation of valvular regurgitation after percutaneous valve repair or replacement: a report from the American Society of Echocardiography Developed in Collaboration with the Society for Cardiovascular Angiography and Interventions, Japanese Society of Echocardiography, and Society for Cardiovascular Magnetic Resonance. *J Am Soc Echocardiogr* 2019; **32**:431–75.
73. Dahou A, Ong G, Hamid N, Avenatti E, Yao J, Hahn RT. Quantifying tricuspid regurgitation severity: a comparison of proximal isovelocity surface area and novel quantitative Doppler methods. *JACC Cardiovasc Imaging* 2019; **12**:560–2.
74. Kebed KY, Addetia K, Henry M, Yamat M, Weinert L, Besser SA et al. Refining severe tricuspid regurgitation definition by echocardiography with a new outcomes-based "Massive" grade. *J Am Soc Echocardiogr* 2020; **33**:1087–94.
75. Bartko PE, Arfsten H, Frey MK, Heitzinger G, Pavo N, Cho A et al. Natural history of functional tricuspid regurgitation: implications of quantitative Doppler assessment. *JACC Cardiovasc Imaging* 2019; **12**:389–97.
76. Muraru D, Previtero M, Ochoa-Jimenez RC, Guta AC, Figliozzi S, Gregori D et al. Prognostic validation of partition values for quantitative parameters to grade functional tricuspid regurgitation severity by conventional echocardiography. *Eur Heart J Cardiovasc Imaging* 2021; **22**:155–65.
77. Ruf TF, Hahn RT, Kreidel F, Beiras-Fernandez A, Hell M, Gerdes P et al. Short-term clinical outcomes of transcatheter tricuspid valve repair with the third-generation MitraClip XTR system. *JACC Cardiovasc Interv* 2021; **14**:1231–40.
78. Badano LP, Hahn R, Rodríguez-Zanella H, Araza Garaygordobil D, Ochoa-Jimenez RC, Muraru D. Morphological assessment of the tricuspid apparatus and grading regurgitation severity in patients with functional tricuspid regurgitation: thinking outside the box. *JACC Cardiovasc Imaging* 2019; **12**:652–64.
79. Qin T, Caballero A, Hahn RT, McKay R, Sun W. Computational analysis of virtual echocardiographic assessment of functional mitral regurgitation for validation of proximal isovelocity surface area methods. *J Am Soc Echocardiogr* 2021; **34**:1211–23.
80. Moraldo M, Cecaro F, Shun-Shin M, Pabari PA, Davies JE, Xu XY et al. Evidence-based recommendations for PISA measurements in mitral regurgitation: systematic review, clinical and in-vitro study. *Int J Cardiol* 2013; **168**:1220–8.
81. Cobey FC, Ashikhmina E, Edrich T, Fox J, Shook D, Bollen B et al. The mechanism of mitral regurgitation influences the temporal dynamics of the vena contracta area as measured with color flow Doppler. *Anesth Analg* 2016; **122**:321–9.
82. Utsunomiya H, Harada Y, Susawa H, Takahari K, Ueda Y, Izumi K et al. Comprehensive evaluation of tricuspid regurgitation location and severity using vena contracta analysis: a color Doppler three-dimensional transeptophageal echocardiographic study. *J Am Soc Echocardiogr* 2019; **32**:1526–37.e2.
83. Sakai K, Nakamura K, Satomi G, Kondo M, Hirotsawa K. Evaluation of tricuspid regurgitation by blood flow pattern in the hepatic vein using pulsed Doppler technique. *Am Heart J* 1984; **108**:516–23.
84. Shapira Y, Porter A, Wurzel M, Vaturi M, Sagie A. Evaluation of tricuspid regurgitation severity: echocardiographic and clinical correlation. *J Am Soc Echocardiogr* 1998; **11**:652–9.
85. Lang RM, Badano LP, Mor-Avi V, Afilalo J, Armstrong A, Ernande L et al. Recommendations for cardiac chamber quantification by echocardiography in adults: an update from the American society of echocardiography and the European association of cardiovascular imaging. *J Am Soc Echocardiogr* 2015; **28**: 1–39.e14.
86. Genovese D, Mor-Avi V, Palermo C, Muraru D, Volpato V, Kruse E et al. Comparison between four-chamber and right ventricular-focused views for the quantitative evaluation of right ventricular size and function. *J Am Soc Echocardiogr* 2019; **32**:484–94.
87. Dietz MF, Prihadi EA, van der Bijl P, Goedemans L, Mertens BJA, Gursoy E et al. Prognostic implications of right ventricular remodeling and function in patients with significant secondary tricuspid regurgitation. *Circulation* 2019; **140**:836–45.
88. Prihadi EA, van der Bijl P, Dietz M, Abou R, Vollema EM, Marsan NA et al. Prognostic implications of right ventricular free wall longitudinal strain in patients with significant functional tricuspid regurgitation. *Circ Cardiovasc Imaging* 2019; **12**:e008666.
89. Park JB, Lee SP, Lee JH, Yoon YE, Park EA, Kim HK et al. Quantification of right ventricular volume and function using single-beat three-dimensional echocardiography: a validation study with cardiac magnetic resonance. *J Am Soc Echocardiogr* 2016; **29**:392–401.
90. Fortuni F, Butcher SC, Dietz MF, van der Bijl P, Prihadi EA, De Ferrari GM et al. Right ventricular-pulmonary arterial coupling in secondary tricuspid regurgitation. *Am J Cardiol* 2021; **148**:138–45.
91. Lurz P, Orban M, Besler C, Braun D, Schlotter F, Noack T et al. Clinical characteristics, diagnosis, and risk stratification of pulmonary hypertension in severe tricuspid regurgitation and implications for transcatheter tricuspid valve repair. *Eur Heart J* 2020; **41**:2785–95.
92. Bartko PE, Hulsmann M, Hung J, Pavo N, Levine RA, Pibarot P et al. Secondary valve regurgitation in patients with heart failure with preserved ejection fraction, heart failure with mid-range ejection fraction, and heart failure with reduced ejection fraction. *Eur Heart J* 2020; **41**:2799–810.
93. Topilsky Y, Inojosa JM, Benfari G, Vaturi O, Maltais S, Michelen H et al. Clinical presentation and outcome of tricuspid regurgitation in patients with systolic dysfunction. *Eur Heart J* 2018; **39**:3584–92.
94. Spinka G, Bartko PE, Heitzinger G, Prausmuller S, Pavo N, Frey MK et al. Natural course of nonsevere secondary tricuspid regurgitation. *J Am Soc Echocardiogr* 2021; **34**:13–9.
95. Bannehr M, Kucken T, Ulrike K, Haase-Fielitz A, Butter C. Prognostic implications of a novel algorithm to grade secondary tricuspid regurgitation. *J Am Soc Echocardiogr* 2021; **34**:1316–7.
96. Fortuni F, Dietz MF, Prihadi EA, van der Bijl P, De Ferrari GM, Knuuti J et al. Prognostic implications of a novel algorithm to grade secondary tricuspid regurgitation. *JACC Cardiovasc Imaging* 2021; **14**:1085–95.



97. Zhan Y, Debs D, Khan MA, Nguyen DT, Graviss EA, Khalaf S *et al*. Natural history of functional tricuspid regurgitation quantified by cardiovascular magnetic resonance. *J Am Coll Cardiol* 2020;**76**:1291–301.
98. Andersen S, Nielsen-Kudsk JE, Vonk Noordegraaf A, de Man FS. Right ventricular fibrosis. *Circulation* 2019;**139**:269–85.
99. Zhan Y, Senapati A, Vejpongsa P, Xu J, Shah DJ, Nagueh SF. Comparison of echocardiographic assessment of tricuspid regurgitation against cardiovascular magnetic resonance. *JACC Cardiovasc Imaging* 2020;**13**:1461–71.
100. Rodes-Cabau J, Hahn RT, Latib A, Laule M, Lauten A, Maisano F *et al*. Transcatheter therapies for treating tricuspid regurgitation. *J Am Coll Cardiol* 2016;**67**:1829–45.
101. Taramasso M, Maisano F. Transcatheter tricuspid valve intervention: state of the art. *EuroIntervention* 2017;**13**:AA40–50.
102. Volpato V, Badano LP, Figliozzi S, Florescu DR, Parati G, Muraru D. Multimodality cardiac imaging and new display options to broaden our understanding of the tricuspid valve. *Curr Opin Cardiol* 2021;**36**:513–24.
103. Caravita S, Figliozzi S, Florescu DR, Volpato V, Oliverio G, Tomaselli M *et al*. Recent advances in multimodality imaging of the tricuspid valve. *Expert Rev Med Devices* 2021;**18**:1069–81.
104. Carpentier A. Cardiac valve surgery—the “French correction”. *J Thorac Cardiovasc Surg* 1983;**86**:323–37.
105. Dreyfus J, Audureau E, Bohbot Y, Coisne A, Lavie-Badie Y, Bouchery M *et al*. TRI-SCORE: a new risk score for in-hospital mortality prediction after isolated tricuspid valve surgery. *Eur Heart J* 2021;ehab679.
106. Fukuda S, Song JM, Gillinov AM, McCarthy PM, Daimon M, Kongsarepong V *et al*. Tricuspid valve tethering predicts residual tricuspid regurgitation after tricuspid annuloplasty. *Circulation* 2005;**111**:975–9.
107. Alfieri O, De Bonis M, Lapenna E, Agricola E, Quarti A, Maisano F. The “clover technique” as a novel approach for correction of post-traumatic tricuspid regurgitation. *J Thorac Cardiovasc Surg* 2003;**126**:75–9.
108. Lapenna E, De Bonis M, Verzini A, La Canna G, Ferrara D, Calabrese MC *et al*. The clover technique for the treatment of complex tricuspid valve insufficiency: midterm clinical and echocardiographic results in 66 patients. *Eur J Cardiothorac Surg* 2010;**37**:1297–303.
109. da Silva JP, Baumgratz JF, da Fonseca L, Franchi SM, Lopes LM, Tavares GM *et al*. The cone reconstruction of the tricuspid valve in Ebstein’s anomaly. The operation: early and midterm results. *J Thorac Cardiovasc Surg* 2007;**133**:215–23.
110. Di Mauro M, Foschi M, Dato GMA, Centofanti P, Barili F, Corte AD *et al*; Italian Group of Research for Outcome in Cardiac Surgery (GIROC). Surgical treatment of isolated tricuspid valve infective endocarditis: 25-year results from a multicenter registry. *Int J Cardiol* 2019;**292**:62–7.
111. Gammie JS, Chu MWA, Falk V, Overbey JR, Moskowitz AJ, Gillinov M *et al*. Concomitant tricuspid repair in patients with degenerative mitral regurgitation. *N Engl J Med* 2021;doi: 10.1056/NEJMoa2115961.
112. Hahn RT, Abraham T, Adams MS, Bruce CJ, Glas KE, Lang RM *et al*. Guidelines for performing a comprehensive transesophageal echocardiographic examination: recommendations from the American Society of Echocardiography and the Society of Cardiovascular Anesthesiologists. *J Am Soc Echocardiogr* 2013;**26**:921–64.
113. Taramasso M, Alessandrini H, Latib A, Asami M, Attinger-Toller A, Biasco L *et al*. Outcomes after current transcatheter tricuspid valve intervention: mid-term results from the international trivalve registry. *JACC Cardiovasc Interv* 2019;**12**:155–65.
114. Besler C, Orban M, Rommel KP, Braun D, Patel M, Hagl C *et al*. Predictors of procedural and clinical outcomes in patients with symptomatic tricuspid regurgitation undergoing transcatheter edge-to-edge repair. *JACC Cardiovasc Interv* 2018;**11**:1119–28.
115. Mehr M, Taramasso M, Besler C, Ruf T, Connelly KA, Weber M *et al*. 1-year outcomes after edge-to-edge valve repair for symptomatic tricuspid regurgitation: results from the trivalve registry. *JACC Cardiovasc Interv* 2019;**12**:1451–61.
116. Lurz J, Rommel KP, Unterhuber M, Besler C, Noack T, Borger M *et al*. Safety and efficacy of transcatheter edge-to-edge repair of the tricuspid valve in patients with cardiac implantable electronic device leads. *JACC Cardiovasc Interv* 2019;**12**:2114–6.
117. Kresoja KP, Rommel KP, Lücke C, Unterhuber M, Besler C, von Roeder M *et al*. Right ventricular contraction patterns in patients undergoing transcatheter tricuspid valve repair for severe tricuspid regurgitation. *JACC Cardiovasc Interv* 2021;**14**:1551–61.
118. Orban M, Wolff S, Braun D, Stolz L, Higuchi S, Stark K *et al*. Right ventricular function in transcatheter edge-to-edge tricuspid valve repair. *JACC Cardiovasc Imaging* 2021;**14**:2477–9.
119. Miura M, Alessandrini H, Alkhdair A, Attinger-Toller A, Biasco L, Lurz P *et al*; TriValve Investigators. Impact of massive or torrential tricuspid regurgitation in patients undergoing transcatheter tricuspid valve intervention. *JACC Cardiovasc Interv* 2020;**13**:1999–2009.
120. Lurz P, Stephan von Bardeleben R, Weber M, Sitges M, Sorajja P, Hausleiter J *et al*. Transcatheter edge-to-edge repair for treatment of tricuspid regurgitation. *J Am Coll Cardiol* 2021;**77**:229–39.